LAWRENCE
LIVERMORE
NATIONAL
LABORATORY

LLNL-JRNL-594072

CO2 in the mantle: melting and solid-solid phase boundaries

A. M. Teweldebrhan, B. Boates, S. A. Bonev

October 23, 2012

Earth and Planetary Science Letters

Disclaimer

CO_2 in the mantle: melting and solid-solid phase boundaries

A. M. Teweldeberhan,[1] B. Boates,[1,2] and S. A. Bonev[1,2]

[1] *Lawrence Livermore National Laboratory, Livermore, CA 94550, USA*
[2] *Department of Physics, Dalhousie University, Halifax, NS, B3H 3J5, Canada*

(Dated: September 20, 2012)

The high temperature phase boundaries of CO_2 in the proximity of the Earth's adiabat are determined using first-principles molecular dynamics simulations based on density functional theory. The melting curve, predicted here up to 71 GPa, and the molecular to polymeric solid phase transition are computed through a phase coexistence approach from free energy calculations. The resulting CO_2 phase IV-phase V-liquid triple point is at 31.8 GPa and 1636 K, in excellent agreement with available experimental data. The Earth's geotherm crosses into the non-molecular phase V near 40 GPa and 2160 K, indicating that free deposits of carbon dioxide in the lower mantle would exist as a polymeric solid. We have also examined the thermodynamic stability of phase V and find no indication that is transforms into a dissociated diamond and oxygen phase at mantle conditions.

PACS numbers: ?61.50.Ks, ?63.20.D-, ?71.15.Pd, ?71.15.Mb

I. INTRODUCTION

Carbon dioxide plays a fundamental role in the physics and chemistry of the Earth's interior and its climate. Carbon enters the mantle during subduction of carbon-bearing minerals - mostly carbonates - at the ocean floors. CO_2 is subsequently released in the mantle (and into the atmosphere during volcanic activity) as a product of decarbonation reactions. At the high pressure (P) and temperature (T) conditions found deep within the earth, CO_2 is known to undergo polymerization transitions both in its solid and liquid states. [1,25,36,43] The solid-solid-liquid and liquid-liquid-solid triple points resulting from these transitions are projected to be in close proximity to the mantle adiabat.[4,6,11–13,25,26] Precise knowledge of the thermodynamic properties of carbon dioxide, including its phase boundaries, is therefore important for determining the chemical reactions taking place within the mantle and the depth at which they take place.

The solid-solid phase transitions in CO_2 have been the subject of numerous theoretical and experimental studies. At low P and T, CO_2 crystallizes into dry ice (phase I – a molecular solid with cubic $Pa\bar{3}$ symmetry).[14] Above 10 GPa, dry ice transforms into the metastable orthorhombic phase III ($Cmca$).[5,15,16] At higher temperatures and comparable pressures, three additional molecular phases have been observed: phase II ($P4_2/mnm$), which is thermodynamically stable in the region of the metastable phase III, phase IV ($R\bar{3}c$), and phase VII ($Cmca$).[3,10,12,17,18] Further compression yields transformations to extended polymeric solids, including an amorphous phase[7,8] at low T, and the finite-temperature phases IV and V (β-cristobalite $I\bar{4}2d$).[1,6,11,19–22,46]

Establishing the phase diagram of CO_2, especially at elevated temperatures, has proven to be rather challenging. A main source of difficulty for both experiment and theory originates from its high degree of metastability[44,45]. As a result, the observed properties are very sensitive to the experimental techniques being used (e.g. for heating) and the P-T phase path being transversed. Thus, the structure of phase V has only recently been established conclusively[22,46] and measurements of the melting are limited to pressures below 35 GPa.[9,10,13,23,24]

The latest experiments[13] project that the melting curve of phase V reaches the mantle adiabat just above 35 GPa, where it ends in a triple point formed by solid phase V, fluid CO_2 and a dissociated C and O_2 phase. According to these projections, solid polymeric CO_2 (phase V) is stable in a very small region within the mantle. At $P > 40$ GPa or depths below 1000 km along the Earth's geotherm it decomposes into carbon and oxygen. The issue of CO_2 stability is critical for determining the oxygen fugacity in the mantle and for understating the formation of diamond and the oxidation of lower-mantle materials.[13]. However, without *in situ* measurements, the interpretation of the experimental data is not straightforward and previous experimental works[4,13,26,27] have led to conflicting conclusions regarding the phase separation of CO_2.

Theoretical predictions of the melting curve are scarce. Recent single-phase calculations starting from liquid CO_2 have provided an estimate for the melting curve up to 140 GPa.[25] According to these data, which are a lower bound to the true melting temperatures, the mantle adiabat enters phase V at P around 60 GPa. Given the complexity of the CO_2 phase diagram in the proximity of the geotherm, it is clear that a more accurate theoretical description of the high temperature phase boundaries is required. Furthermore, the calculations[25] showed that dense liquid carbon dioxide does not phase separate up to 200 GPa and 10,000 K, but the thermodynamic stability of solid phase V has not been examined yet. Accordingly, the purpose of this article is: (1) To predict from first principles the melting curve of carbon dioxide in the region where it crosses the mantle adiabat, as well as the finite-temperature solid-solid phase boundary between the molecular and polymeric phases IV and V; (2) To determine the stability of CO_2-V with respect to C +

O phase separation; and (3) To provide thermodynamic data that would be of use to study the chemical reactions taking place within the Earth.

II. COMPUTATIONAL DETAILS

To compute the melting curve using a solid-liquid coexistence approach, we carried out first principles molecular dynamics (FPMD) simulations using finite-T density functional theory (DFT) with PBE-GGA exchange-correlation[28,29] using the VASP code.[30,31] Our simulations were performed in the canonical ensemble (constant N, V, and, T) using a 0.75 fs ionic time-step and a Nosé-Hoover thermostat.[32,33] Supercells containing 96 atoms were used for the liquid as well as solid phases I and V, while 72 atoms were used for phase IV. All calculations were performed using 4- and 6-electron projector augmented wave (PAW) pseudopotentials[34,35] for the carbon and oxygen atoms, with 1.50 and 1.52 Bohr core radii and a 500 eV planewave cut-off. The accuracy of these pseudopotentials was rigorously tested in our previous work,[36] including comparisons with 1.10 Bohr core radii PAW pseudopotentials for both C and O with a 900 eV planewave cut-off and an all-electron oxygen PAW pseudopotential with a 2000 eV planewave cut-off. The Brillouin zone was sampled at the Γ-point, which gave the desired level of accuracy (∼ meV/atom) when compared with larger **k**-point grids. At each P-T point considered, the solid and liquid phases were equilibrated for 3 ps and continued for an additional 10 ps to gather sufficient statistical information.

To construct finite-temperature phase boundaries between the solid and liquid phases, we computed the Gibbs free energies of each phase at various pressures and temperatures. The Gibbs free energy, $G = \langle U \rangle + \langle P \rangle V - TS$, where $\langle ... \rangle$ represents an ensemble (time) average, is computed using a fixed number of atoms N, volume V, and T from FPMD simulations as follows: $\langle U \rangle = \langle E \rangle + \langle KE \rangle$ is the sum of the Kohn-Sham energy and the kinetic energy of the ions, $P = -dE/dV + Nk_BT/V$, and S is the entropy. The relative stability of the different phases is determined by calculating G as a function of P at fixed T.

The entropy of the solid phases is obtained by integrating the vibrational density of states (VDOS), which is the Fourier transform of the velocity auto-correlation function (VACF). Although anharmonicity is present to a certain extent in the simulated VDOS, a harmonic partition function is used to calculate the entropy. To fully account for anharmonic effects at high temperature, we compute corrections to the free energies obtained from the VDOS using thermodynamic integration (TI).[37] In doing so, FPMD simulations were carried out for a system with a potential energy function of the form: $U(\lambda) = U_0 + \lambda(U_1 - U_0)$, where U_0 is the potential energy of a reference system with a known free energy and U_1 is the potential energy of the system under investigation. Here, λ is a coupling parameter that ranges from zero to unity. The Helmholtz free energy difference between the two systems is given by,

$$\Delta F = \int_0^1 d\lambda \left\langle \frac{\partial U(\lambda)}{\partial \lambda} \right\rangle_{N,V,T,\lambda}. \quad (1)$$

The value of (1) is calculated numerically by performing simulations in a canonical ensemble with a Langevin thermostat while varying the coupling parameter. Values from 0 to 1 in intervals of 0.1 have been used for λ. For a reference system, we have chosen an Einstein crystal with harmonic spring constants fitted to reproduce the Helmholtz free energies obtained from the partial VDOS of C and O atoms. With this choice, equation (1) represents the full anharmonic correction to the TS term computed from the VDOS.

The entropy of liquid CO_2 has been computed by decomposing its partial DOS into solid- and gas-like components for both C and O atoms.[38,39] The solid-like parts of the liquid DOS are integrated using a harmonic approximation as mentioned above and the gas-like parts are treated using a hard-sphere model which includes anharmonicity. This is an approximate but efficient method and its accuracy for mono- and multi-component systems has been examined in refs. 39 and 40.

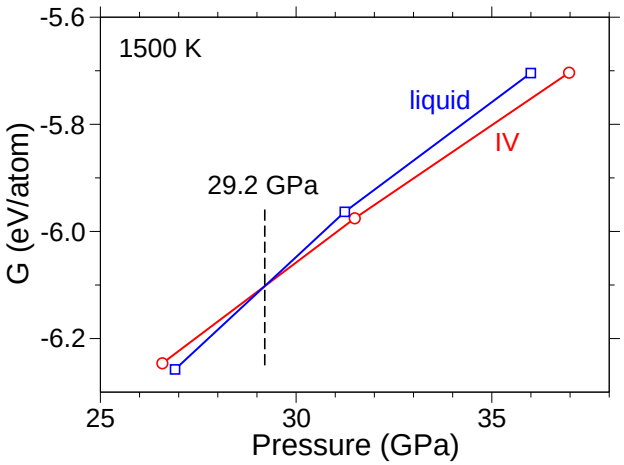

FIG. 1: Pressure dependence of the Gibbs free energy of the liquid (blue squares) and molecular solid phase IV (red circles) at 1500 K. The crossing of the two curves indicates a melting pressure of 29.2 GPa.

III. RESULTS AND DISCUSSION

Fig. 1 shows the Gibbs free energies for the liquid and molecular solid phase IV along the 1500 K isotherm. The crossing at 29.2 GPa indicates the melting pressure at this temperature. The Gibbs free energies for the liquid

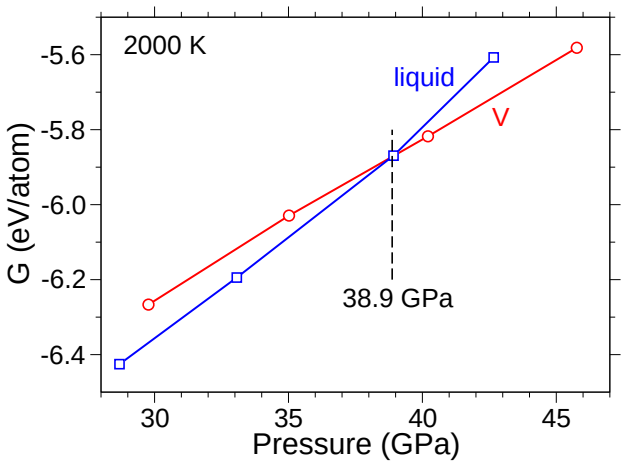

FIG. 2: Pressure dependence of the Gibbs free energy of the liquid (blue squares) and polymeric solid phase V (red circles) at 2000 K. The crossing of the two curves indicates a melting pressure of 38.9 GPa.

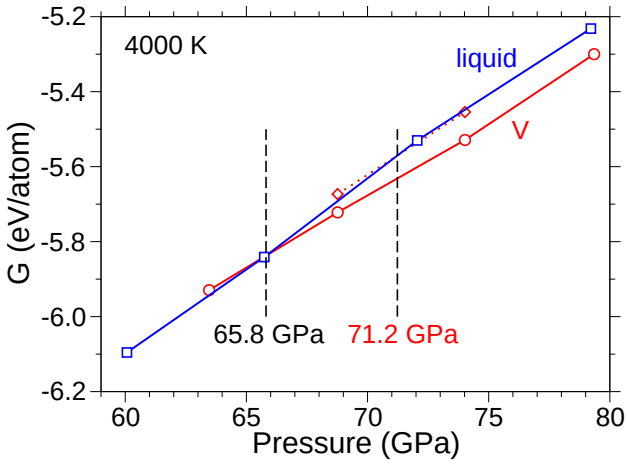

FIG. 3: Gibbs free energy as a function of pressure of liquid (blue squares) and polymeric solid phase V at 4000 K where the entropy of the solid has been computed using the VDOS within a harmonic approximation (red circles and solid line) and with anharmonic corrections obtained from thermodynamic integration (red diamonds with dotted line).

and polymeric solid phase V along the 2000 K isotherm are shown in Fig. 2. The two curves give a melting pressure of 38.9 GPa at 2000 K. The entropies of the solid phases used to compute the free energies in Figs. 1 and 2 were obtained using the VDOS within a harmonic approximation.

Fig. 3 shows the Gibbs free energies for liquid CO_2 and polymeric phase V, indicating melting at 4000 K near 65.8 GPa within a harmonic approximation for the solid entropy. However, at higher-temperatures, the role of anharmonic contributions to the entropy become more important. To investigate the effect of these anharmonic contributions, we have used thermodynamic integration to compute the exact free energy of the solid at high temperature. The decrease in solid entropy when including anharmonic corrections results in a 5.4 GPa increase in the melting pressure at 4000 K (see Fig. 3).

The calculated melting points together with experimental data are summarized in a new P-T phase diagram in Fig. 4. We achieve excellent agreement with experiment for the low-P melting curve calculations and the finite-T phase boundary between phases IV and V. Our predicted liquid-phase IV- phase V triple point at 31.8 GPa and 1636 K also agrees very well with recent experimental measurements ($P = 33 \pm 2$ GPa and $T = 1720 \pm 100$ K) from ref. 13.

The Earth's geotherm (taken from ref. 41) crosses our calculated melting line above 40 GPa and 2160 K and lies below the melting line up to 71 GPa. Therefore, any free deposits of CO_2 deep in the Earth's lower mantle would prefer a polymeric solid state over a fluid one. This may have important implications for our understanding of the rheological weakening and melting of mantle rocks, especially near the core-mantle boundary where fluid CO_2 was thought to play a major role alongside other volatiles.[41,42]

To check the consistency of our melting curve calculations, we have computed the slopes of the solid-liquid transition line using the Clausis-Clapeyron relation:

$$\frac{dP}{dT} = \frac{\Delta H}{T\Delta V}, \qquad (2)$$

where ΔH and ΔV are the differences in enthalpy and volume between the coexisting phases. Equation (2) is solved by interpolating H and V obtained from NVT simulations at each computed melting point. Fig. 4 shows the resulting tangent lines from the Clausis-Clapeyron slopes for our melting curve which appear to be consistent with each neighboring melting point.

Finally, we examine the reported phase separation of CO_2-V into C and O above 40 GPa and 2000 K.[4,13,26] For this purpose, we have computed the Gibbs free energy of mixing between the mixed (CO_2 phase V) and the de-mixed (diamond + ϵ-O_2) phases. These are the phases that have been observed in previous experiments under such conditions. We have computed the Gibbs free energy of mixing per atom ($\Delta G = G_{CO_2} - (G_{diamond} + 2G_{\epsilon-O_2})/3$) near 70 GPa and 3000 K, well above the proposed experimental boundary. Using the VDOS method to compute the entropy of each solid phase, we find we find $\Delta G = -1.01$ eV/atom under these P-T conditions, indicating the mixed state (*i.e.* CO_2 phase V) is thermodynamically preferred. It is worth noting that this large difference in free energies is well outside any uncertainties or approximations in our methods, both numerical and exchange-correlation. The lack of phase separation predicted here is consistent with experimental reports on

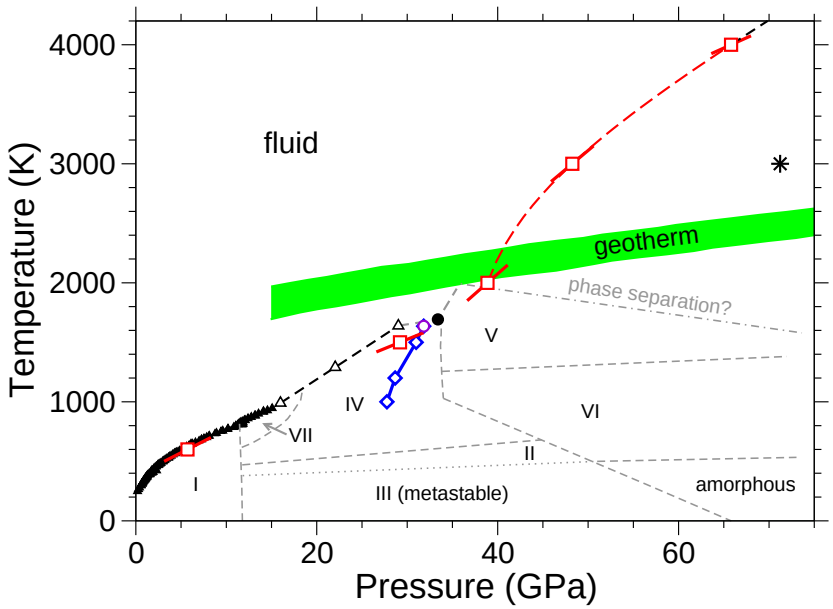

FIG. 4: Computed melting curve points (red squares) and phase IV-V finite-T transition points (blue diamonds). Available experimental data for the melting curve and solid phase boundaries are indicated by black triangles and dashed lines, respectively (experimental triple point is indicated by the black circle).[9,10,13,23,24] Our calculations predict a liquid-phase IV- phase V triple point (purple circle) at 31.8 GPa and 1636 K and a geotherm crossing near approximately 40 GPa and 2160 K. Melting curve slopes were computed at each point using the Clausius-Clapeyron equation (thick red lines). The high-pressure phase-V melting curve (dashed red line) was obtained using a Kechin fit with parameters $a = 2.0983881$ GPa, $b = 0.20921060$, $c = -0.0053306386$ GPa^{-1}, $T_0 = 2000$ K, and $P_0 = 38.872$ GPa.

the decarbonation of compressed $MgCO_3$ into polymeric solid CO_2 with no signs of diamond formation.[27] Moreover, this is also in line with our recent work on high-pressure fluid CO_2.[25]

TABLE I: Computed thermodynamic quantities of liquid and solid (phase V) CO_2 at pressure and temperature conditions found near the the Earth's geotherm. The symbols are defined in the text.

phase	T(K)	P(GPa)	V(A^3/ion)	G(eV/ion)	S(k_B/ion)
Solid	1500	26.58	9.174	-6.2462	5.752
		31.50	8.744	-5.9755	5.662
		36.98	8.399	-5.7036	5.724
Liquid	1500	26.91	9.479	-6.2576	6.702
		31.24	9.084	-5.9634	6.249
		35.00	8.700	-5.7043	6.176
Solid	2000	29.77	6.993	-6.2666	5.319
		35.02	6.829	-6.0291	5.198
		40.21	6.681	-5.8177	5.186
		45.77	6.540	-5.5816	5.097
Liquid	2000	28.69	9.479	-6.4254	7.386
		33.07	9.084	-6.1944	7.393
		38.92	8.700	-5.8693	7.333
		42.66	8.433	-5.6073	6.862

IV. CONCLUSION

We have used FPMD to compute the high-pressure melting curve of CO_2 up to approximately 70 GPa using a solid-liquid phase coexistence approach by calculating finite-temperature free energies of solid and liquid phases. The calculated melting curve and liquid-phase IV-phase V triple point are in very good agreement with available experimental data and are consistent with independently computed Clausis-Clapeyron slopes. We have accurately computed the melting curve crossing of the Earth's geotherm indicating that below 1000 km, free CO_2 present in the lower mantle would exist in a polymeric solid state, having significant implications for geochemical processes such as the melting of mantle rocks. The accuracy of our calculations is verified by the excellent agreement between the computed and measured triple point and the low-P melting curve. We do not observe a transition from the non-molecular solid phase V of CO_2 into a dissociated diamond and oxygen phase. Interesting extensions of this work could include extending the study to even higher pressures or considering the presence of mantle minerals and the effect they may have on the CO_2 melting curve relative to the geotherm.

V. ACKNOWLEDGEMENTS

This work was performed under the auspices of the US Department of Energy (DOE) at the University of California/LLNL under Contract No. DE-AC52-07NA27344. B. Boates and S.A. Bonev acknowledge support from NSERC, Killam Trusts, CFI, and Acenet.

[1] V. Iota, C. S. Yoo, and H. Cynn, Science **283**, 1510 (1999).
[2] J. Dong, J. K. Tomfohr, O. F. Sankey, Phys. Rev. B **62**, 11485 (2000).
[3] V. Iota and C. S. Yoo, Phys. Rev. Lett. **86**, 5922 (2001).
[4] O. Tschauner, H. K. Mao, and R. J. Hemley, Phys. Rev. Lett. **87**, 075701 (2001).
[5] S. A. Bonev, F. Gygi, T. Ogistu, and G. Galli, Phys. Rev. Lett. **91**, 065501 (2003).
[6] M. Santoro, J. F. Lin, H. K. Mao, and R. J. Hemley, J. Chem. Phys. **121**, 2780 (2004).
[7] M. Santoro, F.A. Gorelli, R. Bini, G. Ruocco, S. Scandolo, and W.A. Crichton, Nature **441**, 857 (2006).
[8] J.A. Montoya, R. Rousseau, M. Santoro, F. Gorelli, and S. Scandolo, Phys. Rev. Lett. **100**, 163002 (2008).
[9] V. M. Giordano, F. Datchi, and A. Dewaele, J. Chem. Phys. **125**, 054504 (2006).
[10] V. M. Giordano and F. Datchi, Europhys. Lett. **77**, 46002 (2007).
[11] V. Iota, C. S. Yoo, J. H. Klepeis, Z. Jenei, W. Evans, and H. Cynn, Nat. Mater. **6**, 34 (2007).
[12] F. Datchi, V. M. Giordano, P. Munsch, and A. M. Saitta, Rev. Lett. **103**, 185701 (2009).
[13] K. D. Litasov, A. F. Goncharov, and R. J. Hemley, Earth Planet. Sci. Lett. **309**, 318 (2011).
[14] B. Olinger, J. Chem. Phys. **77**, 6255 (1982).
[15] R. C. Hanson, J. Chem. Phys. **89**, 4499 (1985).
[16] K. Aoki, H. Yamawaki, and M. Sakashita, Phys. Rev. B **48**, 9231 (1993).
[17] C. S. Yoo, V. Iota, and H. Cynn, Phys. Rev. Lett. **86**, 444 (2001).
[18] F. A. Gorelli, V. M. Giordano, P. R. Salvi, and R. Bini, Phys. Rev. Lett. **93**, 205503 (2004).
[19] Y. Seto, D. Nishio-Hamane, T. Nagai, N. Sata, and K. Fujino, J. Phys.: Conf. Ser. **215**, 012015 (2010).
[20] C. S. Yoo, H. Cynn, F. Gygi, G. Galli, V. Iota, M. Nicol, S. Carlson, D. Hausermann, and C. Mailhiot, Phys. Rev. Lett. **83**, 5527 (1999).
[21] J. Dong, J. K. Tomfohr, O. F. Sankey, Phys. Rev. B **61**, 5967 (2000).
[22] F. Datchi, B. Mallick, A. Salamat, and S. Ninet, Phys. Rev. Lett. **108**, 125701 (2012).
[23] P. W. Bridgman, Phys. Rev. **3**, 126 (1914).
[24] J. D. Grace and G. C. Kennedy, J. Phys. Chem. Solids **28**, 977 (1967).
[25] B. Boates, A.M. Teweldeberhan, S.A. Bonev, unpublished
[26] Y. Seto, D. Hamane, T. Nagai, and K. Fujino, Phys. Chem. Minerals **35**, 35 (2008).
[27] N. Takafuji, K. Fujino, T. Nagai, Y. Seto, and D. Hamane, Phys. Chem. Minerals **33**, 651 (2086).
[28] J. P. Perdew, K. Burke, and M. Ernzerhof, Phys. Rev. Lett. **77**, 3865 (1996).
[29] J. P. Perdew, K. Burke, and M. Ernzerhof, Phys. Rev. Lett. **78**, 1396 (1996).
[30] G. Kresse and J. Hafner, Phys. Rev. B **47**, 558 (1993).
[31] G. Kresse and J. Furthmüller, Phys. Rev. B **54**, 11169 (1996).
[32] S. Nosé, J. Chem. Phys. **81**, 511 (1984).
[33] W. G. Hoover, Phys. Rev. A **31**, 1695 (1985).
[34] P. E. Blöchl, Phys. Rev. B **50**, 17953 (1994).
[35] G. Kresse and D. Joubert, Phys. Rev. B **59**, 1758 (1999).
[36] B. Boates, S. Hamel, E. Schwegler, and S.A. Bonev, J. Chem. Phys. **134**, 064504 (2011).
[37] A. M. Teweldeberhan, J. L. DuBois, and S. A. Bonev, Phys. Rev. Lett. **105**, 235503 (2010).
[38] S.-T. Lin, M. Blanco, and W. A. Goddard III, J. Phys. Chem. B **119**, 11792 (2003).
[39] S.-T. Lin, P. K. Maiti, and W. A. Goddard III, J. Phys. Chem. B **114**, 8191 (2010).
[40] A. M. Teweldeberhan and S. A. Bonev, Phys. Rev. B **83**, 134120 (2011).
[41] M. Isshiki, T. Irifune, K. Hirose, S. Ono, Y. Ohishi, T. Watanuki, E. Nishibori, M. Takata, and M. Sakata, Nature **427**, 60 (2004).
[42] R. Dasgupta and M.M. Hirschmann, Nature **440**, 659 (2006).
[43] S. Serra, C. Cavazzoni, G. L. Chiarotti, S. Scandolo, and E. Tosatti, Science **284**, 788 (1999).
[44] M. Santoro and F. A. Gorelli, Phys. Rev. B **80**, 184109 (2009).
[45] A. Sengupta and C.S. Yoo, Phys. Rev. B **82**, 012105 (2010).
[46] M. Santoro *et al.* Proc. Nat. Acad. Sci. **109**, 14808 (2012).